

The $K\alpha$ complex of He-like iron with dielectronic satellites

Justin Oelgoetz¹ and Anil K. Pradhan²

¹ *Department of Chemistry,* ² *Department of Astronomy, The Ohio State University, Columbus, OH 43210, USA*

Accepted xxxxxx Received xxxxxx; in original form xxxxxx

ABSTRACT

It is shown that the dielectronic satellites (DES) dominate X-ray spectral formation in the 6.7 keV $K\alpha$ complex of Fe XXV at temperatures below that of maximum abundance in collisional ionization equilibrium T_m . Owing to their extreme temperature sensitivity the DES are excellent spectral diagnostics for $T < T_m$ in photoionized, collisional, or hybrid plasmas; whereas the forbidden, intercombination, and resonance lines of Fe XXV are not. A diagnostic line ratio $GD(T)$ is defined including the DES and the lines, with parameters from new relativistic atomic calculations. The DES *absorption* resonance strengths may be obtained from differential oscillator strengths to possibly yield the Fe XXIV/Fe XXV column densities. The DES contribution to highly ionized Fe should be of interest for models of redward broadening of $K\alpha$ features, ionized accretion discs, accretion flows, and $K\alpha$ temporal-temperature variability in AGN.

Key words: Atomic Processes – Atomic Data – X-ray: K-shell – line:profiles – galaxies:Seyfert – X-rays:galaxies

1 INTRODUCTION

The $K\alpha$ features are complexes of lines from K-shell transitions. Fe $K\alpha$ lines are prominent in the X-ray spectra of AGN, with associated photon energies that range from the so called ‘neutral iron’ 6.4 keV fluorescent feature from Fe I-Fe XVI, up to 6.7 and 6.9 keV from highly ionized He- and H-like Fe XXV and Fe XXVI. The observed $K\alpha$ features from a number of AGN and quasars appear to peak at these energies (e.g. Nandra *et al.* 1997). The highly ionized Fe XXVI/Fe XXV X-ray emission may serve as possible diagnostics of accretion flows and the structure of the source plasma (Naryayan and Raymond 1999). The nature of the accretion flow on to the black hole or neutron star may determine whether the plasma is photoionization or collisionally dominated, with distinct X-ray signatures. The X-ray spectra of a number of AGN exhibit a long redward tail down to almost 5 keV (e.g. Tanaka *et al.* 1995, Nandra *et al.* 1997), attributed to relativistic broadening of the emitting radiation from the close proximity to the black hole. Accretion disc models assumed an essentially ‘neutral’ plasma, with a peak at 6.4 keV. The new *Chandra* observations show a narrow $K\alpha$ feature of ionized Fe from the well known AGN NGC 5548 (Yaqoob *et al.* 2001). Recently models have been proposed with ionized Compton reflection from the inner region of the accretion disc, and including separate diskline components (Ballantyne and Fabian 2001). The 6.7 keV complex of Fe XXV may constitute part of these highly ionized Fe components. X-ray variability of Fe $K\alpha$ emission has also

been observed, for example, on rapid timescales in NGC 7314 (Yaqoob *et al.* 1996), but constant over long time intervals from the AGN MCG–6-30-15 6 with some evidence of short time scale variations indicating possible flaring activity (Lee *et al.* 2000). As described in this work, the $K\alpha$ complex is sensitive to both the temperature and the ionization state, but the spectral diagnostics needs to include the dielectronic satellites. It is of interest to study precisely the basic physics of spectral formation of highly ionized Fe that might discriminate between the atomic and the astrophysical processes.

As first noted by Gabriel and Jordan (1969), and followed by other studies (e.g. Mewe and Schrijver 1978a,b, Pradhan and Shull 1981, Bely-Dubau *et al.* 1982), He-like ions provide powerful X-ray diagnostics. There is a set of forbidden (f), intercombination (i), and resonance (r) lines dependent on plasma parameters such as temperature, density, and ionization state. The spectroscopic and laboratory designations for these lines are: w,x,y,z, corresponding to the 4 transitions to the ground level $1s^2$ (1S_0) \leftarrow $1s2p(^1P_1^o)$, $1s2p(^3P_2^o)$, $1s2p(^3P_1^o)$, $1s2s(^3S_1)$ respectively. For temperatures $T < T_m$, in recombination dominated non-coronal plasmas it has been shown that (e + ion) recombination preferentially enhances the triplet (x,y,z) lines and hence the ratio $G = (x+y+z)/w$, which may be thereby employed as diagnostics of both the temperature and the ionization state (Pradhan 1982, 1985). Since recombinations depend on the ionization fraction of H-like to He-like ratio $X_H = \text{Fe XXVI}/\text{Fe XXV}$, recombination

dominated photoionized plasmas may be accordingly modeled (Liedahl 2000, Porquet and Dubau 2000, Bautista and Kallman 2000).

The dielectronic satellites (DES) are generally formed due to *emission* from autoionizing levels – an excited ion level with a quasi-bound electron. The (e + ion) system may autoionize in a radiationless transition, or stabilise (dielectronic recombination) via radiative decay with a photon of wavelength redward of the ‘resonance’ line (w) at 6.696 keV. Recently X-ray photoabsorption in KLL resonances of Li-like O VI was predicted (Pradhan 2000), and detected in the *Chandra* observations of MCG–6-30-15 (Lee *et al.* 2001). Together with other observed photoabsorption and emission lines redward of the resonance lines of H- and He-like O, and Fe L-shell spectra, this helps in the spectral discrimination between a ‘dusty warm absorber’ model and alternative models of relativistically broadened $K\alpha$ lines (Branduardi-Raymont *et al.* 2001). The O VI and O VII column densities were also determined from the same X-ray observations (Lee *et al.* 2001) using the computed O VI(KLL) resonance oscillator strengths (Pradhan 2000, Nahar *et al.* 2001a). The DES photoabsorption calculations have now been extended to the KLL resonances of (e + C V) and (e + Fe XXV) (Nahar *et al.* 2001a). In this *Letter* we examine the role of DES in the $K\alpha$ complex of Fe XXV, both in emission and absorption, and point out potentially useful diagnostics.

2 THEORY AND COMPUTATIONS

A brief description of the characteristics of the principal line ratios and the DES based on previous laboratory, astrophysical, and theoretical studies is given below.

2.1 The principal lines w,x,y,z

All He-like ions provide diagnostic line ratios involving the principal lines from the bound levels of the ground and $n = 2$ configurations, $R = z/(x+y)$ and $G = (x+y+z)/w$, that usually depend on density and temperature respectively. Furthermore, one can establish numerical limits on the ratio G that indicate the ionization state of the plasma: $G \approx 1 \rightarrow$ collisional (coronal) ionization equilibrium; $G > 1 \rightarrow$ recombination dominated (photoionization or hybrid); $G < 1 \rightarrow$ ionization dominated. Among the first examples of observed non-ionization equilibrium plasmas were: the recombination dominated laboratory tokamak spectra by Källne *et al.* (1984), the *Einstein* X-ray spectra of ionization dominated plasmas in SNR’s Puppis A (Winkler *et al.* 1981) and the Cygnus Loop (Vedder *et al.* 1986), and in the laboratory tokamak spectra under rapid time-dependent ionization (Lee *et al.* 1985,1986).

2.2 The dielectronic satellites KLL and KLn ($n > 2$)

Unlike elements lighter than iron, the DES in Fe are comparably strong relative to the principal lines, even for $T \approx T_m$ in collisional equilibrium, such as in tokamak plasmas (Bitter *et al.* 1981), in Electron Beam Ion Traps (EBIT, Beiersdorfer *et al.* 1992), and in the solar corona and flares

(e.g. Kato *et al.* 1998). The autoionizing levels responsible for DES are excited by electrons at precisely the energies corresponding to those levels. The DES are therefore more sensitive to the electron distribution (Maxwellian or non-Maxwellian) than the principal lines which are excited by all electrons at energies above the excitation threshold. Moreover, the DES are spread over a much wider range in energy.

Following Gabriel (1972), several researchers have computed the DES intensities (e.g. Bhalla *et al.* 1975, Bely-Dubau *et al.* 1979, 1982, Karim and Bhalla 1992, Vainshtein and Safronova 1978). To our knowledge, the most recent calculations of DES intensities is by Pradhan and Zhang (1997), from highly resolved fine structure photoionization cross sections of Fe XXIV including radiation damping of autoionizing resonances (Nahar *et al.* 2001a). These constitute a part of new relativistic atomic calculations for photoionization, recombination, and transition probabilities of Fe XXV (Zhang *et al.* 1999, Nahar and Pradhan 1999, Nahar *et al.* 2001b) using the Breit-Pauli R-matrix (BPRM) method (Hummer *et al.* 1993, Berrington *et al.* 1995). Photoionization and recombination are treated self-consistently using an identical eigenfunction expansion for the system (e + Fe XXV) \rightleftharpoons Fe XXIV for the two inverse processes, based on a unified method for (e + ion) recombination that subsumes both the radiative and the dielectronic recombination (RR and DR) processes in an ab initio manner (e.g. Zhang *et al.* 1999). The computed autoionization and radiative rates for Fe XXV are given in Table 1 of Pradhan and Zhang (1997) for all DES of the $n = 2$ KLL (1s2s2p) complex, labelled according to the standard notation ‘a-v’ and their spectroscopic designations (Gabriel 1972). The higher- n DES, $3 \leq n \leq 10$ (KLM, KLN,.....,KLT) are also similarly calculated (the $n > 2$ contribution is negligible). The BPRM DES(KLL) strengths agree to within 10 - 20% of the EBIT experimental measurements, and with other works; the DES(KLn, $n > 2$) are in similar agreement with Bely-Dubau *et al.* (1979). Recombination-cascade coefficients for (w,x,y,z) are from Mewe and Schrijver (1978), and collisional rates from Pradhan (1985); collisional rates for ISE DES are from Kato *et al.* (1995).

3 RESULTS AND DISCUSSION

While details of the calculations will be reported in a subsequent paper, we describe briefly the main theoretical results relevant to spectral analysis of observations with blended principal and DES features.

3.1 Line ratios and dielectronic satellites

Fig. 1 shows the $K\alpha$ complex of Fe XXV including the (w,x,y,z) lines and the DES(KLL) at a range of temperatures from $\text{Log}(T) = 6.8 - 7.8$ (the line profiles are thermally broadened). The various panels in Fig. 1 reveal the large temperature variations and the dominance of the DES intensities relative to the (w,x,y,z) up to $T \approx 3 \times 10^7$ K ($< T_m$). He-like ions span the largest temperature range of any ionization state; T_m (Fe XXV) $\approx 10^{3.5-5.0}$ in coronal equilibrium (Arnaud and Raymond 1992). The DES may be further sub-divided according to inner-shell excitation (ISE)

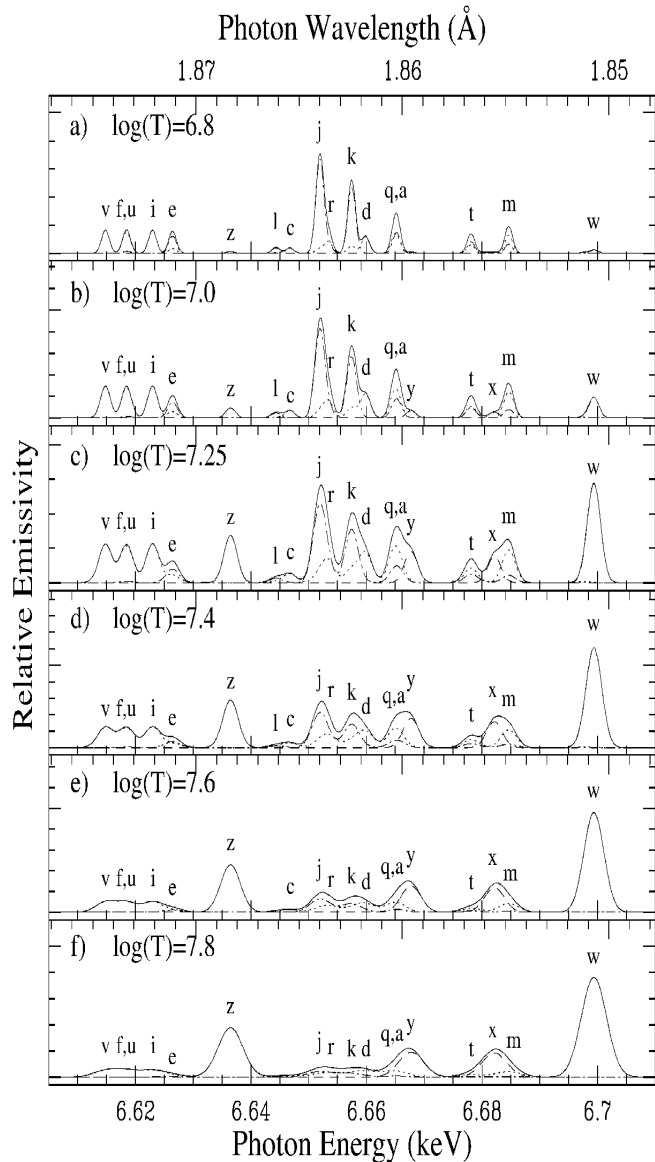


Figure 1. Fe XXV($K\alpha$) spectra vs. $\text{Log}(T) = 6.8 - 7.8$; solid line - sum of principal lines w,x,y,z, and the DES(KLL); dashes - (w,x,y,z); dotted - ISE satellites; dot-dash - DR satellites. The features are thermally broadened.

from Li-like Fe XXIV (dotted, Fig. 1), and (e + ion) dielectronic recombination (DR) of (e + Fe XXV) (dash-dot, Fig. 1). For $T \geq T_m$ the w-line is predominant since the large fraction of electrons in the Maxwellian tail contribute to its intensity relative to all other lines.

It is readily seen from Fig. 1 that the G ratio is no longer a useful one for He-like iron. This is not only due to the relative weakness of the principal lines, but also blending with the DES with different temperature dependences. Furthermore, the contribution of $n \geq 3$ DES to the w-line needs to be considered. We obtain the higher- n satellite intensities KL_n ($2 < n \leq 10$, i.e. KLM, KLN, etc.), from the BPRM calculations as in Table 2 of Zhang *et al.* (1999). The DES(KL_n , $n > 2$) can not be resolved from the w-line by current X-ray observatories. We assume that the DES(KLL)

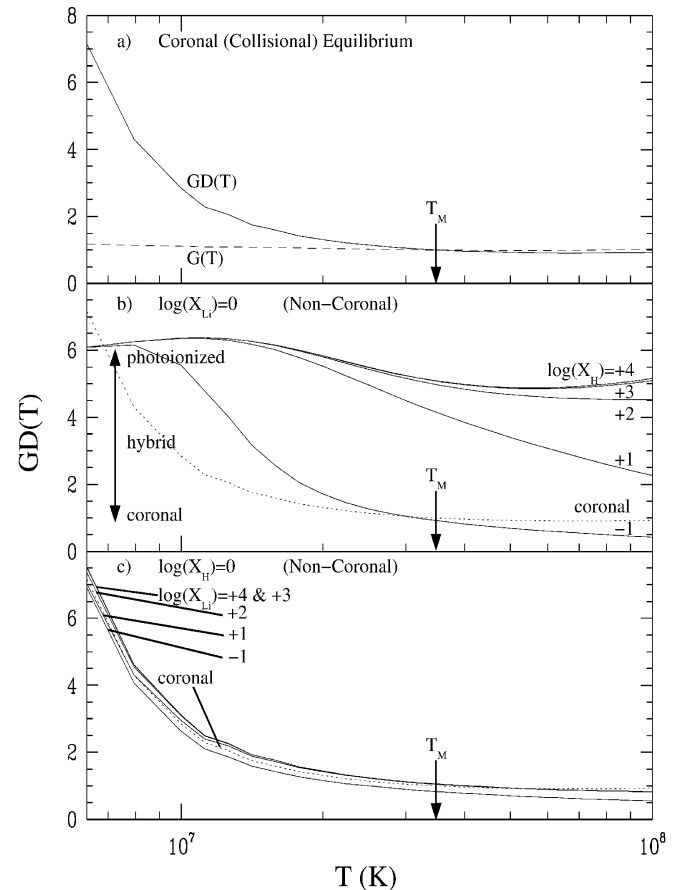


Figure 2. The ratio $GD(T)$ in Eq. 1: a) in coronal equilibrium, compared to $G(T)$; b) non-coronal $GD(T)$ variation in recombination dominated plasmas with $X_H = N(\text{Fe XXVI})/N(\text{Fe XXV})$; c) $GD(T)$ variation with $X_{Li} = N(\text{Fe XXIV})/N(\text{Fe XXV})$.

intensity may be measured, albeit blended with the (x,y,z) lines, relative to the w-line blended with the higher- n satellites. Therefore we re-define the G ratio, including DES, as

$$GD \equiv (x + y + z + KLL) / (w + \sum_{n>2} KL_n) \quad (1)$$

Fig. 2a shows $GD(T)$ compared with $G(T)$ in coronal equilibrium. Whereas the latter shows practically no variation, the $GD(T)$ increases by up to a factor of 7 compared to $G(T)$ at the lower end of the temperature range $\approx 6 \times 10^6$ K, and compared to $T \geq T_m$. Therefore in photoionized plasmas, or in otherwise low- T recombination dominated plasmas, the ratio $GD(T)$ should be a good diagnostics of temperature with a limiting value $GD(T \ll T_m) \rightarrow KLL / \sum_{n>2} KL_n$.

The DES blending and dominance implies however that $GD(T)$ will not be as good a diagnostic of ionization state for He-like Fe as for lighter elements. The DES are largely independent of ionization state; the DR satellites depend only on Fe XXV, and the relative intensities of (w,x,y,z) are smaller. The non-coronal cases are illustrated in Figs. 2b and 2c. Fig. 2b shows the variation of $GD(T)$ with H-like to He-like ionization fraction X_H in completely recombination dominated plasmas ($X_{Li} \rightarrow 0$). Fig. 2c shows the variation with respect to the Li-like to He-like ionization fraction X_{Li}

in plasmas ionizing through Fe XXIV ($X_H \rightarrow 0$). Unlike the recombination dominated case in Fig. 2b, the temperature dependences in Figs. 2a (coronal equilibrium) and 2c are similar, since in both cases the DES dominate at lower T, and collisional excitation of (w,x,y,z) at higher T. The non-coronal recombination dominated case in Fig. 2b is similar to $G(T)$ for all He-like ions, since recombinations populate only the bound levels that lead preferentially to (x,y,z) emission, and not autoionizing levels that yield the DES. The curves in Fig. 2b are therefore similar to that by Porquet and Dubau (2000) who considered He-like ions of elements up to Si, but where the DES are relatively inconsequential. As in Fig. 2a, the Bautista and Kallman (2000) results for He-like Fe including the DES also show a sharp rise in $G(T)$ as T decreases; however they present values only for $G \leq 2.5$, and therefore it is difficult to discern whether there is quantitative agreement with the present results.

As with the G ratio, the density sensitive ratio $R = z/(x+y)$ is not likely to provide accurate diagnostics for Fe XXV, since the DES blends with different types of ISE and DR satellites will introduce temperature and ionization-state dependence in R as well. Nonetheless, a more detailed analysis of all components of the $K\alpha$ complex (i.e. Fig. 1) might enable calculations of the R, including the DES, in cases with sufficient observational resolution ($\Delta \lambda < 0.01 \text{ \AA}$).

3.2 The total $K\alpha$ (Fe XXV) intensity

The total intensity $I(K\alpha)$ vs. T is plotted in Fig. 3 (relative units), showing the relative contributions of DES and principal lines: $I(KLL)$, $I(KLn, n > 2)$, and $I(w+x+y+z)$. We note that: (i) $I(KLL) \approx I(K\alpha)$ for $T \leq 10^7$ K, i.e. the DES(KLL) constitute almost the entire $K\alpha$ intensity, (ii) the DES (KLL + $\sum_{n>2} KLn$) continue to dominate $K\alpha$ up to 3×10^7 K (and hence the temperature dependence of $GD(T)$ in Fig. 2a), and (iii) For $T > T_m$ the DES are weaker and the principal lines approach $G(T)$. The inset in Fig. 3 shows $I(K\alpha)$ on a different scale, with the peak values and the relative ionic abundances of Fe XXIV, Fe XXV, and Fe XXVI vs. T. The maxima of $K\alpha$ (Fe XXV) components do not coincide with the Fe XXV peak abundances $N_{Fe\ XXV}(T_m)$; rather, the intensities also depend on adjacent ionization states and the DES. It bears emphasis that under non-equilibrium, time-dependent, rapidly variable plasma conditions the line ratios and the DES may vary widely in intensity. Thus we expect a strong and sensitive temporal-temperature variation of the entire $K\alpha$ complex.

3.3 Absorption spectra of the DES(KLL)

Finally, in Fig. 4 we consider the *absorption* spectra in the KLL satellites due to X-ray photoabsorption from Fe XXIV. As mentioned earlier, we have calculated differential oscillator strengths, $\frac{df}{d\epsilon}$, for the KLL resonances in He-like C,O, and Fe from highly resolved relativistic photoionization cross sections (Nahar *et al.* 2001a). Fig. 4 shows the detailed $\frac{df}{d\epsilon}$ with the spectral energy absorption across the ISE DES profiles. Integration over the individual profiles yields the \bar{f}_r , the resonance oscillator strengths that may be used in a completely analogous manner as the line f -values (Pradhan 2000). At 1.860 \AA we may predict a strong absorption

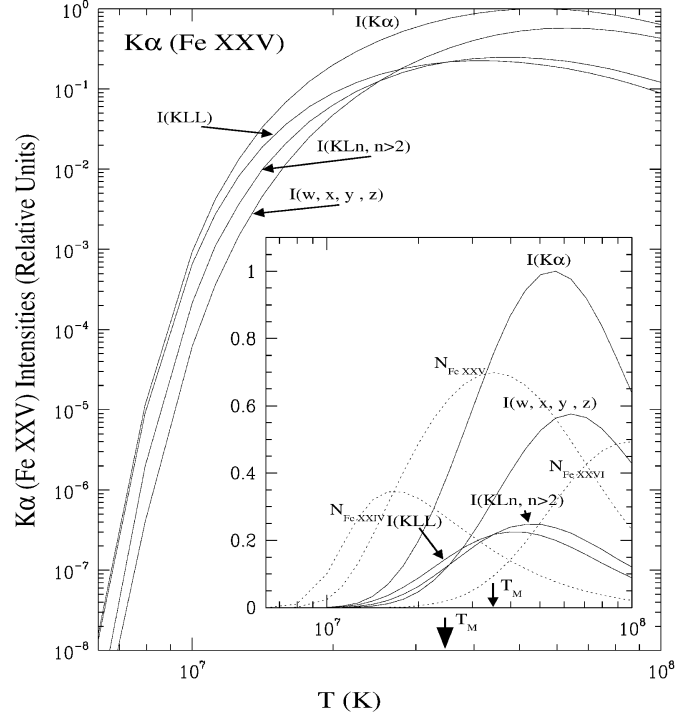


Figure 3. $K\alpha$ (Fe XXV) intensity, with $I(KLL)$, $I(KLn, n > 2)$, and $I(w,x,y,z)$; the inset is on different scale, also showing relative coronal equilibrium abundances. As shown, the DES dominate $K\alpha$ intensity for $T < T_m$.

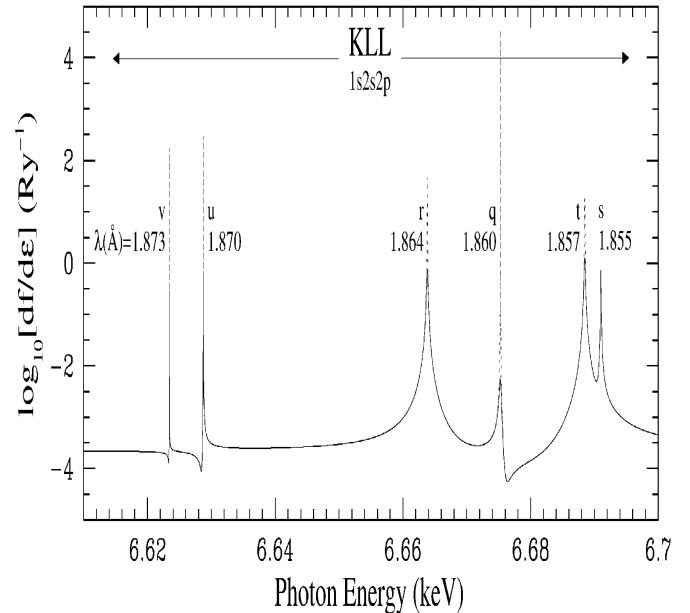


Figure 4. Fe XXIV KLL differential oscillator strengths with resolved X-ray spectral features (adapted from Nahar *et al.* 2001a). The solid lines are radiatively damped values, and the dashed lines are undamped values appropriate for optically thin plasmas.

feature due largely to the ‘q’ ISE satellite (and to a lesser extent from the ‘r’ and ‘t’), with $\bar{f}_r = 0.75$ (0.044) (from Table 1, Nahar *et al.* 2001a). The two \bar{f}_r values correspond to radiatively undamped and damped values (dashed and solid lines); the former is appropriate for optically thin plasmas with little re-emission along the line of sight. If the 1.86 Å feature is resolvable from the λ (w) at 1.85 Å of Fe XXV ($f(w) = 0.703$), then, in principle, Fe XXIV/Fe XXV column densities may be determined from measured equivalent widths using curves-of-growth. However, that may not be feasible due to y-line emission also at 1.86 Å, and other DES. Nonetheless, X-ray *absorption* in the DES (ISE) needs to be considered in $K\alpha$ spectral analysis.

4 CONCLUSION

The main results are:

1. The highly ionized 6.7 keV Fe XXV component of Fe $K\alpha$ emission is dominated by the DES. Those from H-like Fe XXVI should similarly contribute at ~ 6.9 keV. Resonance and satellite line emission from lower ionization states of Fe should manifest itself down to 6.4 keV.
2. The DES appear redward of the w-line, and should be largely undiminished by resonance scattering unlike the w-line; therefore the observed $K\alpha$ features might appear redshifted.
3. The principal line ratios G and R from the $n = 2$ excited levels involving the lines (w,x,y,z) are not reliable diagnostics for Fe XXV due to DES strengths and blending. A new ratio GD(T) is defined including the DES.
4. Owing to the predominance of DES the $K\alpha$ complex may exhibit considerable temperature sensitivity, and hence possible temporal variability in AGN.
5. K-shell DES *absorption* may be considered using ‘resonance oscillator strengths’ \bar{f}_r to determine column densities and ionic fractions.

ACKNOWLEDGMENTS

We would like to thank Hong Lin Zhang for the data on high- n DES, and Sultana Nahar for the $\frac{df}{de}$ (KLL) data. This work was partially supported by the U.S. National Science Foundation and NASA Astrophysical Theory Program. The computational work was carried out at the Ohio Supercomputer Center in Columbus Ohio.

REFERENCES

Arnaud, M. & Raymond, J., 1992, ApJ, 398, 394
 Ballantyne, D.R. & Fabian, A.C., 2001, MN (preprint, astro-ph/0104342)
 Bautista, M.A. & Kallman, T.W., 2000, ApJ, 544, 581
 Beiersdorfer, P., Philips, T.W., Wong, K.L., Marrs, R.E., Vogel, D.A. 1992, Phys. Rev. A 46, 3812
 Bely-Dubau, F., Gabriel, A.H., Volonte, S., 1979, MNRAS, 189, 801
 Bely-Dubau, F., Dubau, J., Faucher, P., Gabriel, A.H. 1982, Mon. Not. R. Roy. Astro. Soc. 198, 239
 Berrington, K.A., Eissner, W., Norrington, P.H., 1995, Comput. Phys. Commun. , 92, 290

Bhalla, C.P., Gabriel, A.H., Presnyakov, L.P., 1975, MNRAS, 172, 359
 Bitter, *et al.* , 1981, Phys. Rev. Letts., 47, 921
 Branduardi-Raymont, G., Sako, M., Kahn, S.M., Brinkamn, A.C., Kaastra, J.S., Page, M.J., 2001, A&A, 365, L140
 Gabriel, A.H. 1972, MNRAS , 160, 99
 Gabriel, A.H. & Jordan, C 1969, MNRAS , 145, 241
 Hummer, D.G., Berrington, K.A., Eissner, W., Pradhan, A.K., Saraph, H.E., Tully, J.A., 1993 A&A , 279, 298
 Källne, E., Källne, J., Dalgarno, A., Marmar, E.S., Rice, J.E., Pradhan, A.K., 1984, Phys. Rev. Letts., 52, 2245
 Karim, K.R. & Bhalla, C.P., 1992, Phys. Rev. A , 45, 3932
 Kato, T., Safronova, U., Shlyaptseva, A., Cornille, M., Dubau, J., 1995, NIFS-DATA-24, National Institute for Fusion Science, Nagoya 464-01, Japan.
 Kato, T., Fujiwara, T., Hanaoka, Y., 1998, ApJ, 492, 822
 Lee, J., Fabian, A.C., Christopher, S.R., Brandt, W.N., Iwasawa, K., 2000, MNRAS, 318, 857
 Lee, J., *et al.* , 2001 (in press, astro-ph/0101065)
 Lee, P., Lieber, A., Chase, R.P., Pradhan, A.K., 1985, Phys. Rev. Letts., 55, 386
 Liedahl, D.A. 2000, in *Atomic data needs in X-ray astronomy*, Eds. M.A. Bautista, T. R. Kallman, A.K. Pradhan, NASA Publications, (<http://heasarc.gsfc.nasa.gov/docs/heasarc/atomic/proceed.html>)
 Mewe, R. & Schrijver, 1978, A&A, 65, 99
 Nahar, S.N. & Pradhan, A.K., 1992, Phys. Rev. Letts. , 68, 1488 (NP1)
 Nahar, S.N. & Pradhan, A.K., 1999, A&AS , 135, 347
 Nahar, S.N., Pradhan, A.K., Zhang, H.L., 2001a, Phys. Rev. A , Rapid Commun., 63, 060701-1
 Nahar, S.N., Pradhan, A.K., Zhang, H.L., 2001b, ApJS, 133, 255
 Nandra, K., George, I.M., Mushotzky, R.F., Turner, T.J., Yaqoob, T., 1997, ApJ, 477, 602
 Narayan, R. & Raymond, J., 1999, ApJ, 515, L69
 Porquet, D. & Dubau, J., 2000, A&AS, 143, 495
 Pradhan, A.K. 1982, ApJ, 263, 477
 Pradhan, A.K. 1985, ApJ, 288, 824
 Pradhan, A.K. 2000, ApJ, 545, L165
 Pradhan, A.K. & Shull, J.M., 1981, ApJ, 249, 821
 Pradhan, A.K. & Zhang, H.L., 1997, J. Phys. B , 30, L571
 Tanaka, T. *et al.* , 1995, Nature, 375, 659
 Vedder, P.W., Canizares, C.R., Markert, T.H., Pradhan, A.K., 1986, ApJ, 307, 269
 Vainshtein, L.A. & Safronova, U.I., 1978, ADNDT, 25, 49
 Winkler, P.F., Clark, G.W., Markert, T.H., Petre, R., Canizares, C.R., 1981, ApJ, 245, 574
 Yaqoob, T. George, I.M., Nandra, K., Turner, T.J., Serlemitsos, P., Mushotzky, R.F.
 Yaqoob, T., Serlemitsos, P.J., Turner, T.J., George, I.M., Nandra, K., 1996, ApJ, 470, L27
 Zhang, H.L., Nahar, S.N., Pradhan, A.K., 1999. J. Phys. B , 32, 1459